IEEE Access
Multidisciplinary ⋮ Rapid Review ⋮ Open Access Journal

Received 21 April 2026, accepted 8 May 2026. Date of publication 00 xxxx 0000, date of current version 00 xxxx 0000.

Digital Object Identifier 10.1109/ACCESS.2026.3693377

Modeling Energy Consumption Impact of Autonomous Vehicles at Pedestrian Crossings Considering Pedestrian-Aware Speed Adaptation

SZILÁRD SZIGETI[1,2], GÁBOR PAUER[2], AND DÁVID FÖLDES[1]
[1]Department of Transport Technology and Economics, Faculty of Transport Engineering and Vehicle Engineering, Budapest University of Technology and Economics, 1111 Budapest, Hungary
[2]KTI Institute for Transport Sciences, 1119 Budapest, Hungary

Corresponding author: Szilárd Szigeti (szigeti.szilard@edu.bme.hu)

Project no. KDP-IKT-2023-900-I1-00000957/0000003 has been implemented with the support provided by the Ministry of Culture and Innovation of Hungary from the National Research, Development and Innovation Fund, financed under the KDP-2023 funding scheme.

ABSTRACT Pedestrian crossings are critical locations in urban traffic networks where frequent deceleration and acceleration strongly influence vehicle energy consumption. The increasing presence of autonomous vehicles creates new opportunities to optimize vehicle approach behavior in such environments; however, the combined effects of automation level and vehicle propulsion technology remain insufficiently explored. This study presents a microsimulation-based framework developed in Vissim traffic simulation software to evaluate energy consumption at unsignalized pedestrian crossings under mixed traffic conditions, considering both internal combustion engine and electric vehicles. The framework integrates pedestrian movement, vehicle dynamics, and a pedestrian-aware speed-adaptation logic implemented via an external scripting interface. Human-driven vehicles are represented using multiple driving behavior profiles, while autonomous vehicles dynamically adjust their speed based on pedestrian position and detection range. Energy consumption is calculated using physics-based formulations, enabling a consistent comparison across propulsion types. A comprehensive set of scenarios was analyzed by varying autonomous vehicle penetration rates and pedestrian detection capabilities. Results indicate that increasing automation reduces energy consumption by approximately 3–7% at low to medium penetration levels and by about 12% under fully autonomous traffic conditions. These improvements are primarily driven by smoother speed adaptation and reduced abrupt deceleration, while statistical analysis confirms that autonomous vehicle penetration is the dominant influencing factor. Similar relative reductions are observed for both propulsion types, with differences remaining within approximately one percentage point across the analyzed scenarios. Overall, the findings demonstrate that pedestrian-aware autonomous driving can significantly improve energy efficiency at pedestrian crossings.

INDEX TERMS Autonomous vehicles, pedestrian-aware speed adaptation, electric vehicles, energy consumption, mixed traffic, pedestrian crossing, microsimulation.

I. INTRODUCTION

Road transport is a major contributor to greenhouse gas (GHG) emissions in the European Union, accounting for 73.2% of transport-related emissions and 28.9% of total GHG emissions in 2022 [1]. Transport has also been the only sector in which emissions increased over the past three decades, rising by 33%. Despite stricter emission standards and growing adoption of electric vehicles, overall transport-related emissions have not declined and are projected to increase further as traffic demand grows. According to the EU Reference Scenario, passenger transport demand is expected to grow by 40% and freight by nearly 60% between 2010 and 2050 [2], [3]. These trends pose significant challenges to decarbonization objectives and highlight the need for additional mitigation strategies beyond vehicle electrification alone.

The associate editor coordinating the review of this manuscript and approving it for publication was Tuan Anh Le.

Autonomous vehicles (AVs) offer opportunities to mitigate environmental impacts by enabling smoother traffic flow, reducing unnecessary acceleration and braking, and improving operational efficiency. Although the development of AVs is increasingly associated with electric propulsion systems, both internal combustion engine vehicles and electric vehicles are expected to coexist in traffic systems during a prolonged transition period, particularly in mixed traffic environments. Consequently, understanding the energy implications of AV behavior across different propulsion technologies remains an important research challenge. Previous studies suggest that high levels of automation could substantially reduce system-level GHG emissions; for example, Patella et al. [4] estimated reductions of up to 60% under full automation scenarios. Beyond environmental benefits, AVs are expected to enhance road safety [5], [6], [7], improve traffic efficiency [8], [9], and reshape urban spaces by reducing parking demand [10]. However, the overall impact of AVs remains uncertain, particularly in mixed traffic conditions, where AVs and human-driven vehicles (HDVs) interact.

While numerous studies have examined AV-human interactions and fuel consumption in mixed traffic environments [11], [12], limited attention has been given to unsignalized pedestrian crossings. At these locations, frequent deceleration and acceleration events strongly influence vehicle energy consumption. Existing research has focused primarily on highways [13], platooning scenarios [14], or signalized intersections [15], [16], leaving a gap in understanding AV behavior in pedestrian-dominated urban environments. Moreover, speed-adaptation strategies that explicitly consider pedestrian movement and their implications for vehicle energy use and emissions remain insufficiently explored. Beyond urban traffic, pedestrian trajectory prediction and movement modeling have also been investigated in other shared environments, such as public buildings [17], [18].

This study addresses these gaps by developing a microscopic simulation framework that dynamically links pedestrian movement with AV speed-control logic and evaluates energy consumption under mixed traffic scenarios. The framework integrates pedestrian dynamics and vehicle kinematics using Vissim traffic simulation software, complemented by an external Python-based algorithm, allowing the comparative analysis of internal combustion engine vehicles and electric vehicles under identical traffic control conditions.

The remainder of this paper is organized as follows. Section II reviews related work, Section III describes the proposed methodology, Section IV outlines the simulation scenarios, Section V presents and discusses the results, and Section VI concludes the paper with key findings and directions for future research.

II. LITERATURE REVIEW

This section reviews relevant literature on AVs with a focus on energy and emission impacts in mixed traffic, pedestrian–vehicle interactions, and propulsion-related energy modeling. The reviewed studies provide the context for the proposed simulation framework and highlight the remaining research gaps addressed in this paper.

A. ENERGY CONSUMPTION IN MIXED TRAFFIC

Previous studies have extensively examined the impacts of AVs on traffic flow efficiency, fuel consumption, and emissions in mixed traffic environments. Many studies report that automation can smooth traffic flow by reducing unnecessary acceleration and braking, thereby improving energy efficiency. Eco-driving strategies and optimized longitudinal control have been shown to reduce fuel consumption by approximately 10–20% in mixed traffic scenarios [9], [19]. Similar benefits have been reported when adaptive cruise control and cooperative driving strategies are introduced, particularly at higher penetration rates of autonomous or connected vehicles [12], [20].

Several studies emphasize that the magnitude—and in some cases even the direction—of energy and emission impacts strongly depends on traffic composition and control strategy. While low penetration rates of AVs may stabilize traffic flow, conservative autonomous driving behavior can lead to increased fuel consumption under certain conditions [21], [22]. In contrast, higher penetration levels, especially when combined with connectivity or cooperative control, have been associated with notable reductions in fuel consumption and emissions [23], [24]. These findings indicate that the energy impacts of AVs cannot be generalized without considering interaction dynamics with HDVs and the specific autonomous driving logic applied.

Research has also examined the energy impacts of AVs in specific traffic contexts, such as highways, intersections, and platooning scenarios. Studies focusing on highway environments and vehicle platoons have reported fuel savings ranging from approximately 5% to over 20%, depending on control strategy and traffic conditions [25]. At signalized intersections, trajectory optimization and autonomous eco-driving strategies have demonstrated even larger reductions in fuel consumption and emissions [15], [26]. However, these traffic environments differ fundamentally from pedestrian-influenced urban road segments, where frequent speed adjustments are driven by interactions with vulnerable road users rather than traffic control devices.

To provide an overview of existing approaches, Table 1 summarizes representative studies investigating energy consumption and emission impacts of AV-related control strategies across different traffic contexts. The table highlights the diversity of methodologies, traffic environments, and reported energy benefits, and serves as a reference point for positioning the focus of this study.

B. PEDESTRIAN-AWARE SPEED CONTROL

Pedestrian crossings introduce complex interaction dynamics that strongly influence vehicle speed profiles and energy use, particularly in urban environments. For AVs, pedestrian

TABLE 1. Overview of energy and emission impacts of autonomous vehicle control strategies.

Research focus	Methodology	Traffic characteristics	Key findings	Reference
Route planning	ACC based on MPC and DP	CAV	-7.8% energy consumption	[27]
Route planning	Dynamic multi-objective eco-routing strategy	Mixed traffic	-43% GHG and -18.58% NOx	[11]
Traffic system optimization	Simulation-based system-level analysis	Mixed traffic	-34% CO2 emission	[28]
Car-following	nonlinear model predictive control	Mixed traffic	-18.26% fuel consumption	[19]
Car-following	HDV, ACC, CACC car-following models, numerical simulation	Mixed traffic	-24.33% HC, -27.06% NOx, -37.53% CO	[12]
Cooperative ramp merging	V2C Digital Twin	CAV	-7.46% CO2, -31.21% CO, -20% NOx	[29]
Lane management optimization	Drive cycle simulations	Mixed traffic	-47-60% fuel consumption	[30]
Roundabout	Traffic simulation (SUMO)	Mixed traffic	-3.3-22.2% fuel consumption and -6.4-55% CO	[31]
Driving style optimization	Driving cycle analysis (WLTC-3)	CACC	-2.2% fuel consumption	[32]
Driving style optimization	Driving cycle modification simulation	Conventional vehicles	-20% fuel consumption	[9]
Driving style optimization	Eco-driving optimal control	Urban traffic	-10-21% energy consumption	[33]
Driving style optimization	Target headway and speed optimization	Mixed traffic	-10% fuel consumption	[18]
Platooning	Trajectory planning, speed optimization	Mixed traffic	-9.5% fuel consumption	[34]
Platooning	Cooperative Adaptive Cruise Control, VSP model	CAV	-3.8% CO2 and -4% NOx	[35]
Eco driving considering traffic light	DP to solve robustness optimization problem	CAV	-40% fuel consumption	[15]
Eco driving considering traffic light	Optimal speed profile	CAV	-51.8% fuel consumption	[25]
Eco driving considering traffic light	Deep Reinforcement Learning	CAV	-20% CO2 emission	[36]
Eco driving considering traffic light	DRL-based	CAV	-19% energy consumption	[37]
On-ramp merging	Ordinary optimal control method	CAV	26.5-43.5% fuel consumption reduction	[38]

Acronyms: ACC: Adaptive Cruise Control, CACC: Cooperative Adaptive Cruise Control, CAV: Connected Autonomous Vehicles, V2C: Vehicle to Cloud communication, MPC: Model Predictive Control, DP: Dynamic Programming, DRL: Deep Reinforcement Learning.

presence requires adaptive speed control strategies that balance safety and traffic efficiency. As a result, numerous studies have investigated pedestrian–vehicle interactions in the context of autonomous driving, primarily focusing on perception, decision-making, and motion planning.

Existing research has addressed pedestrian detection, intent prediction, and collision avoidance strategies to ensure safe AV operation near crossings [39], [40], [41]. More recent work has explored predictive and learning-based approaches, including trajectory optimization and deep reinforcement learning, to enable anticipatory speed adaptation based on pedestrian movement [42], [43], [44].

While these studies improve safety and traffic performance, energy and emission impacts are rarely evaluated explicitly. Moreover, most analyses focus on isolated AV behavior and neglect mixed traffic interactions with pedestrians and HDVs. As a result, the energy implications of pedestrian-aware speed adaptation remain largely unexplored.

C. COMPARATIVE ANALYSIS OF AUTONOMOUS VEHICLE CONTROL STRATEGIES

Beyond individual vehicle maneuvers, the effectiveness of AV energy-saving logic depends on the broader control paradigm and its interaction with the environment. While established strategies, such as signal-phase-based eco-driving, rely on real-time Signal Phase and Timing (SPaT) data from smart infrastructure to minimize idling at intersections [45], our approach is fully decentralized and operates solely on on-board sensor data.

Recent studies emphasize that in complex, unsignalized urban scenarios, decentralized behavioral adaptation is vital for efficiency [46], [48]. For instance, intent-based trajectory planning can ensure safety in shared spaces [47], while trust-aware advisory systems can optimize the energy use of platoons through collective perception [14]. However, many of these solutions require V2X communication or coordinated fleet data. Our proposed pedestrian-aware strategy distinguishes itself by focusing on autonomous perception-reaction cycles at pedestrian crossings, enabling a stand-alone deployment in urban environments where V2X infrastructure is currently absent. Table 2 provides a functional benchmark of our method against these dominant AV control paradigms.

D. ENERGY IMPACTS OF VEHICLE PROPULSION

Vehicle propulsion technology fundamentally influences how traffic dynamics translate into energy consumption and emissions. Existing studies indicate that smoother speed profiles and reduced stop-and-go behavior—achieved

TABLE 2. Comparison of AV control strategies.

Strategy type	Communication req.	Data Source	Key Advantage	Ref.
Eco-driving (V2I)	High (V2I)	SPaT/V2P	Global flow opt.	[45]
Urban AV Flow	None	Road data	Macro-scale gain	[46]
Intent-based	None	On-board perception	Safe interaction	[47]
Behavioral	None	Simulation	Driving style-opt.	[48]
Cooperative	Med. (V2V)	Fleet data	Platoon stability	[14]
Our proposed method	None	On-board sensors	Stand-alone deployment	

through eco-driving, car-following optimization, or cooperative control—can yield measurable energy savings under diverse traffic conditions [12], [15], [20].

With the increasing adoption of electric vehicles, recent studies emphasize that electrification fundamentally alters the relationship between traffic dynamics and energy use. Higher drivetrain efficiency, negligible idling losses, and regenerative braking lead to different energy responses to speed fluctuations compared to fuel-based vehicles. Simulation-based investigations report that speed-oriented control strategies can reduce electric energy consumption in urban traffic, although the magnitude of the benefit depends strongly on traffic conditions and modeling assumptions [28], [33].

Much of the recent autonomous driving literature implicitly assumes electric propulsion, reflecting current development trends. However, since internal combustion engine vehicles still dominate today's vehicle fleet, there is a clear need to evaluate identical autonomous speed-control logic for both propulsion types in order to make comparable results.

III. METHODOLOGY

A. SIMULATION ENVIRONMENT AND NETWORK CONFIGURATION

A microscopic traffic simulation model was developed using PTV Vissim (version 2024.0.13). Vissim was selected for its ability to model detailed pedestrian–vehicle interactions in urban environments and to support real-time external control of vehicles via the COM interface. AV behavior was controlled by an external Python script, enabling the implementation of a custom speed adaptation logic during the simulation. The simulation time step was set to 0.2 s, providing sufficient temporal resolution for modeling speed adjustments near pedestrian crossings.

The modeled network represents an unsignalized pedestrian crossing on an urban road segment with one lane per direction. The geometry was based on a real pedestrian crossing located at Szőlő Street 80, Budapest, Hungary. While the physical layout reflects this location, the simulation was not calibrated to reproduce site-specific traffic conditions, and no real-world traffic flow data were used for calibration. Representative synthetic traffic and pedestrian volumes were applied to create a controlled environment (ceteris paribus). This approach isolates the energy-impact mechanisms of the AV logic from local demand fluctuations, ensuring that the findings are generalizable to similar urban crossing geometries. The simulation model relies on the Wiedemann 74 car-following model and standard Vissim urban driving parameters, ensuring realistic vehicle interactions without site-specific calibration. Fig. 1 illustrates the modeled road segment and the pedestrian crossing layout.

Each approach to the pedestrian crossing included a 155 m upstream segment to allow AVs to apply detection and speed adaptation logic before reaching the crossing. Downstream of the crossing, an additional 80 m segment was modeled to capture post-crossing acceleration behavior. This configuration ensured that both deceleration and recovery phases were fully represented within the entire simulation horizon.

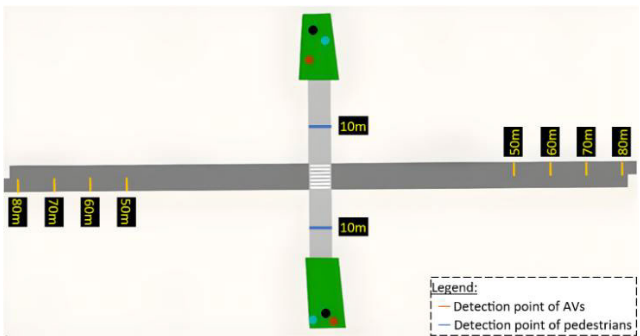

FIGURE 1. Layout of the modeled simulation network at the unsignalized pedestrian crossing.

B. AUTONOMOUS VEHICLE SPEED CONTROL LOGIC

AV behavior at the unsignalized pedestrian crossing was controlled by a rule-based speed-adaptation logic implemented in an external Python script and executed through Vissim's COM interface (the source code is available in the data repository [49]). The purpose of the external script was to enable pedestrian-aware speed adaptation by processing real-time simulation data and issuing speed commands at each simulation timestep. As illustrated in Fig. 2, the control logic operates as part of a broader simulation framework in which vehicle and pedestrian data are exchanged between Vissim, the external control module, and the energy and emission calculation components.

At each simulation timestep, the Python script executed a sequence of operations summarized in Fig. 3.

In Step 1, pedestrian-related data were retrieved, including walking direction, walking speed, and remaining distance to the crossing. In Step 2, vehicle-related data were obtained for the approaching AV, including vehicle type, speed, lane, and distance to the crossing. These inputs provided the basis for evaluating potential pedestrian–vehicle interactions in the vicinity of the crossing.

In Step 3, the presence of pedestrians within a predefined 10 m detection area around the crossing was evaluated. If no pedestrian was detected within this area, the AV maintained its desired approach speed (Step 4). Pedestrian detection was applied exclusively to AVs. HDVs were not equipped with pedestrian awareness or adaptive speed control.

If a pedestrian was detected, the control logic proceeded with conflict assessment. In Step 5, pedestrian crossing times were estimated by computing the time required to reach the crossing, the midpoint, and to fully clear the crossing. The midpoint was included to capture direction-dependent yielding behavior. For pedestrians approaching from the near side, the AV logic allowed the vehicle to proceed once the pedestrian has reached the road centerline, as the vehicle could safely pass behind them. To ensure safety, a 0.5 second safety buffer was added behind the pedestrian before the AV reached the crossing. For pedestrians approaching from the far side, the AV yielded until the pedestrian had fully cleared the crossing. In Step 6, the applicable vehicle detection distance—50, 60, 70, or 80 m upstream of the crossing—was selected based on the predefined AV sensing configuration. These distances served as simplified proxies for different levels of AV sensing capability. While real-world sensors are influenced by stochastic environmental factors, this approach ensures comparable conditions across scenarios. This allows the isolation of how sensing range influences speed adaptation and energy consumption. In Step 7, the remaining distance of the approaching AV to the pedestrian crossing was calculated, followed by computation of the corresponding vehicle arrival time in Step 8.

In Step 9, pedestrian and vehicle arrival times were compared to determine whether a potential conflict existed at the crossing. If a conflict was identified, Step 10 determined the critical pedestrian crossing time based on the applicable yielding rule, and in Step 11, the optimal AV speed was calculated to ensure safe and comfortable yielding behavior. Once the pedestrian had reached the relevant clearance point—either the midpoint or the far-side curb, depending on crossing direction—the AV resumed acceleration toward its desired speed, subject to vehicle performance limits.

This decision-making sequence—covering pedestrian detection, time-to-crossing estimation, conflict assessment, and speed adjustment—was executed repeatedly at each simulation timestep to ensure continuous responsiveness to pedestrian movements.

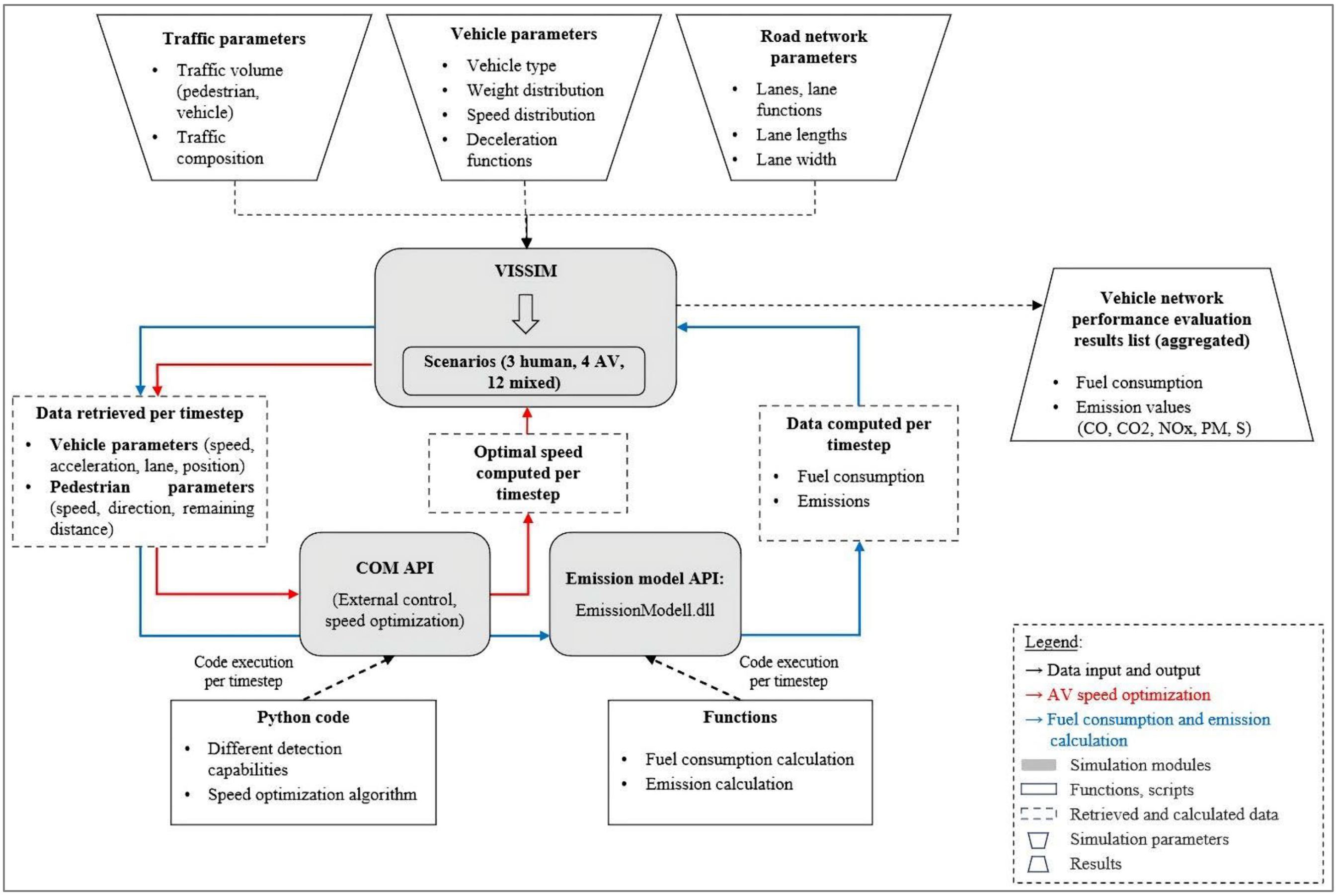

FIGURE 2. Structural and operational framework of the Vissim –Python-External-Emission Model (EEM) based simulation model.

C. ENERGY CONSUMPTION AND EMISSION MODELING

Energy consumption and emission impacts were evaluated using Vissim's External Emission Model (EEM), which computes vehicle energy use based on instantaneous vehicle dynamics generated by the microscopic traffic simulation. The emission model operates independently of the traffic control logic and relies on vehicle trajectories—specifically speed and acceleration profiles—produced by the simulation. This separation ensures that differences in energy outcomes originate from traffic behavior and propulsion characteristics rather than from changes in the control logic itself.

1) EXTERNAL EMISSION MODEL FRAMEWORK

Within the EEM, energy demand is computed using user-defined, vehicle-dynamics-based formulations. We implemented the total tractive force (F_t) required at the wheels at each simulation timestep, which was obtained as the sum of resistive forces and inertial effects, and is expressed as:

$$F_t = F_r + F_d + F_a \tag{1}$$

where F_r denotes rolling resistance, F_d the aerodynamic drag, and F_a the inertial force associated with vehicle acceleration.

The rolling resistance force is calculated as:

$$F_r = c_r \cdot m \cdot g \tag{2}$$

where c_r is the rolling resistance coefficient, m the vehicle mass, and g the gravitational acceleration.

Aerodynamic drag is expressed as:

$$F_d = 1/2 \cdot \rho \cdot c_d \cdot A \cdot v^2 \tag{3}$$

where ρ is air density, c_d the aerodynamic drag coefficient, A the vehicle frontal area, and v the vehicle speed.

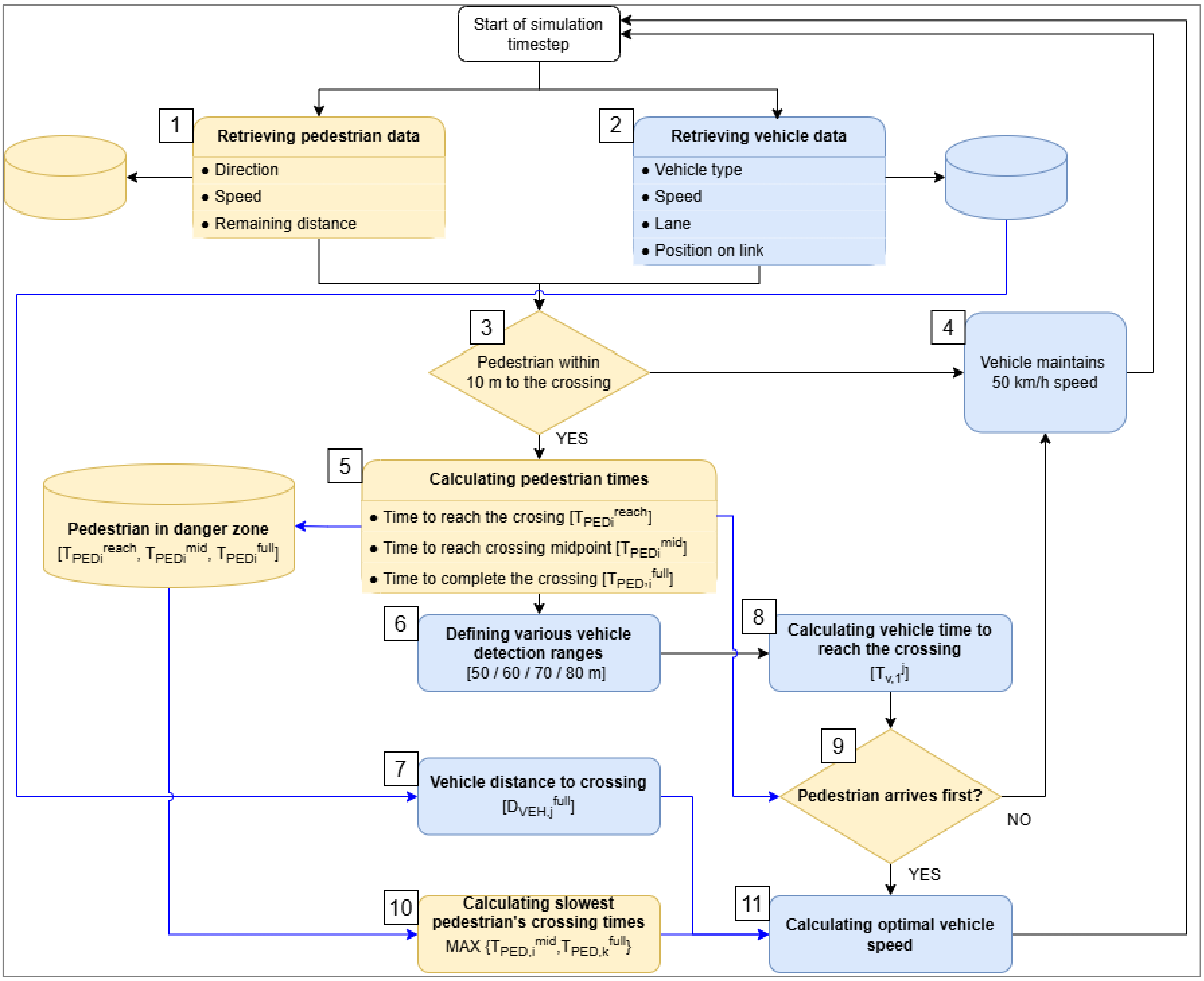

FIGURE 3. Timestep-based pedestrian-aware speed control logic for autonomous vehicles.

The inertial force associated with longitudinal acceleration is given by:

$$F_i = m \cdot a \tag{4}$$

where a denotes the longitudinal acceleration of the vehicle.

Based on the total tractive force, the instantaneous tractive power demand P_t is computed as:

$$P_t = F_t \cdot v \tag{5}$$

The resulting power demand values are evaluated at each simulation timestep and passed to the propulsion-specific energy calculation described in Sections III-C.2 and III-C.3.

2) INTERNAL COMBUSTION ENGINE VEHICLES

For ICE vehicles, the instantaneous fuel consumption rate is derived from the tractive power demand and engine efficiency characteristics. Fuel consumption $\dot{f}$ is calculated as:

$$\dot{f} = \frac{P_t}{\eta_{ICE} \cdot H_f} \tag{6}$$

where η_{ICE} is the overall drivetrain efficiency and H_{f} is the lower heating value of the fuel.

The total fuel consumption is obtained by integrating the instantaneous fuel flow over the 1-hour simulation horizon. To allow comparison across scenarios with different traffic realizations, aggregated fuel use is normalized and reported in liters per 100 km.

3) ELECTRIC VEHICLES

Electric vehicles (EVs) were modeled in EEM using the same trajectory-based framework, with propulsion-specific energy conversion applied within the emission model. The instantaneous electrical power demand P_{e} is calculated as:

$$P_e = \frac{P_t}{\eta_{EV}} \tag{7}$$

where P_{t} denotes the tractive power demand and η_{EV} represents the electric drivetrain efficiency.

During deceleration phases, negative tractive power values correspond to braking events. The regenerated electrical power (P_{regen}) through regenerative braking is computed as:

$$P_{regen} = \eta_{regen} \cdot |P_t| \; for \; P_t < 0 \tag{8}$$

where η_{regen} signs the regenerative braking efficiency. Negative tractive power values corresponding to braking are interpreted as regenerated electrical energy and are deducted from net electrical energy consumption.

The total electrical energy consumption (E_{EV}) is obtained by integrating the net electrical power over the simulation timeframe:

$$E_{EV} = \int \left(P_e - P_{regen}\right) dt \tag{9}$$

Aggregated electrical energy consumption values were normalized and reported in kilowatt-hours per 100 km to enable comparison across different traffic scenarios. As the same speed-control logic and vehicle trajectories were applied to all vehicle types, differences in electric vehicle energy consumption arise solely from propulsion characteristics and traffic dynamics.

IV. SIMULATION PARAMETERS AND SCENARIOS

This section describes the simulation setup and scenario design applied in the study. The objective of this section is to provide a transparent and reproducible overview of the applied vehicle-related parameters, traffic and scenario configurations, and propulsion-specific assumptions, thereby enabling a consistent interpretation of the energy consumption and emission results presented in the subsequent sections.

A. VEHICLE-RELATED PARAMETERS AND SPEED ASSUMPTIONS

The vehicle-related control and behavior parameters applied in the simulation, including speed assumptions, braking characteristics, and pedestrian detection capabilities for HDVs and AVs are summarized in Table 3. To represent variability in human driving behavior, three HDV driving styles (cautious, normal, and aggressive) were defined based on their deceleration characteristics. These driving profiles were applied only in fully human-driven baseline scenarios, while mixed-traffic scenarios used a single representative (normal) driving style to isolate the effects of AV penetration.

TABLE 3. Vehicle-related parameters and control assumptions.

Parameter	Human-driven vehicles (HDV)	Autonomous vehicles (AV)
Speed assumption – Case 1	48-58 km/h (distributed)	50 km/h (fixed)
Speed assumption – Case 2	50 km/h (fixed)	50 km/h (fixed)
Desired deceleration (m/s^2)	-2.0 / -2.75 / -3.5 (cautious / normal / aggressive)	-2.0
Maximum deceleration (m/s^2)	-5.5 / -7.0 / -8.0	-7.0
Pedestrian detection capability	Not available	50 / 60 / 70/ 80 m

Two speed-setting cases were applied exclusively to HDVs. In Case 1, HDVs followed Vissim's default speed distribution between 48 and 58 km/h, In Case 2, HDVs were constrained to a fixed speed of 50 km/h. AVs, however, operated with a fixed speed of 50 km/h in both cases. Their speed could only be modified dynamically by the pedestrian- aware control logic. The second case was introduced to isolate the effects of pedestrian-aware speed adaptation from differences caused solely by human speeding behavior. To ensure comparability across the simulated AV penetration levels, the speed distribution of HDVs was kept consistent regardless of the AV traffic share.

In addition to speed setting assumptions, pedestrian detection capability was considered as a key characteristic of AV operation near the pedestrian crossing. Based on reported pedestrian detection ranges and sensing system capabilities in the literature [50], [51], [52], AV detection distances were parameterized at 50, 60, 70, and 80 m.

B. SIMULATION ENVIRONMENT AND STOCHASTIC DESIGN

All scenarios were simulated using the same unsignalized pedestrian crossing geometry described in Section III. Traffic demand and pedestrian flow were kept constant across all simulations to ensure comparability between scenarios. Vehicle traffic volume was set to 200 vehicles per hour per direction, while pedestrian demand was fixed at 200 pedestrians per hour per direction.

Pedestrian walking speeds were fixed to provide a controlled environment for isolating the impact of AV penetration and sensing range on energy consumption. Male pedestrians were assigned a walking speed of 4.7 km/h, while female pedestrians walked at 4.0 km/h. The simulation duration was set to one hour, with a simulation timestep of 0.2 seconds.

To account for stochastic variability in traffic interactions, each simulation scenario was executed five times using different random seeds (7, 12, 21, 30, and 42). Reported results represent average values across these independent simulation runs.

The main simulation-related parameters are summarized in Table 4.

TABLE 4. Simulation-related parameters.

Category	Value / Description
Simulation duration	1 hour
Simulation time step	0.2 s
Vehicle demand	200 veh/hour per direction
Pedestrian demand	200 ped/hour per direction
Pedestrian walking speed	4.7 km/h (male), 4.0 km/h (female)
Pedestrian conflict zone	10 m around the crossing
Stochastic realizations	5 runs per scenario (random seeds: 7, 12, 21, 30, 42)

C. PROPULSION MODELING AND EMISSION CONVERSION

Each simulation scenario was evaluated using ICE and electric propulsion models, while traffic dynamics and vehicle control logic were kept identical. This approach allowed the isolation of propulsion-related effects from traffic- and behavior-related influences.

Each traffic scenario was simulated separately using ICE and EV propulsion models. No mixed ICE–EV fleet was applied; the entire vehicle population was modeled as either 100% ICE or 100% EV, while HDV/AV ratios remained identical across propulsion types.

Vehicle mass was specified at the vehicle-class level. ICE vehicles were assigned a mass range of 1200–1800 kg, while EVs were assigned a higher range of 1400–2400 kg, reflecting typical differences between the two powertrain technologies.

ICE vehicles were modeled with a drivetrain efficiency of 0.25 and a fuel heating value of 33.7 MJ/L [53]. EVs were assigned a drivetrain efficiency of 0.85 and a regenerative braking efficiency of 0.65 [54], [55], [56], [57], [58], [59]. Regenerative braking was limited to 50 kW and disabled at vehicle speeds below 2.0 m/s [59], [60]. Aerodynamic and rolling resistance parameters were identical for both propulsion types.

Emission impacts were evaluated exclusively for gasoline-powered ICE vehicles using a fuel-based emission factor approach, as EVs have no tailpipe emissions during vehicle operation. Fuel consumption values obtained from the simulation were converted from liters to kilograms using a conversion factor of 0.74 kg/L [61]. Pollutant emissions were then calculated by multiplying the consumed fuel mass by constant emission factors for CO, CO_2, NO_x, PM, and sulphur, following the EEA emission inventory guidelines [62]. As emission calculations were directly proportional to fuel consumption, relative emission changes across scenarios followed the same trends as fuel consumption results.

The key energy and emission model (EEM) parameters were selected to be representative for current vehicle technologies, ensuring that all values fall within the ranges identified in the existing literature. These EEM parameters, along with their respective references are summarized in Table 5. While absolute energy results are sensitive to specific powertrain calibrations, using fixed parameters ensures a consistent baseline for a controlled comparison of AV-related impacts.

TABLE 5. Powertrain-related parameters for ICE and EV vehicles.

Parameter	Internal combustion engine vehicles (ICE)	Electric vehicles (EVs)	Reference
Vehicle mass range (kg)	1200-1800	1400-2400	[63]
Drivetrain efficiency	0.25	0.85	[54], [55]
Regenerative braking efficiency	-	0.65	[56], [57]
Maximum regenerative power	-	50 kW	[58], [59]
Minimum speed for regeneration	-	2.0 m/s	[60]
Frontal area (m^2)	2.3	2.3	[64]
Rolling resistance coefficient	0.01	0.01	[65,64]
Aerodynamic drag coefficient	0.3	0.3	[65]
Fuel heating value	33.7 MJ/L	-	[53]

D. SCENARIO MATRIX

The simulation scenarios were designed to systematically examine the effects of traffic composition, AV penetration, and pedestrian detection capability on energy consumption and emissions near an unsignalized pedestrian crossing. A total of nineteen scenarios were defined by combining different proportions of HDVs and AVs with multiple AV detection ranges.

AV penetration levels of 0%, 25%, 50%, 75%, and 100% were investigated. Fully HDV-based scenarios included cautious, normal, and aggressive driving behaviors. In mixed traffic scenarios, AVs were combined exclusively with normal HDVs in order to limit scenario dimensionality and isolate the effects of automation and sensing capability.

The complete set of simulated scenarios is summarized in Table 6.

TABLE 6. Scenario matrix of simulated traffic compositions and sensing configurations.

Scenario	Traffic composition	AV detection range [m]
1	100 % HDVs - cautious	-
2	100 % HDVs - normal	-
3	100 % HDVs - aggressive	-
4-7	75% HDVs (normal) + 25% AVs	50, 60, 70, 80
8-11	50% HDVs (normal) + 50% AVs	50, 60, 70, 80
12-15	25% HDVs (normal) + 75% AVs	50, 60, 70, 80
16-19	100% AVs	50, 60, 70, 80

In total, the experimental design consisted of 19 traffic composition scenarios, 2 propulsion types (ICE and EV), 2 speed-setting cases, and 5 stochastic realizations per configuration. This resulted in 380 independent simulation runs (19 × 2 × 2 × 5), ensuring statistical robustness of the reported results.

V. RESULTS

This section presents the simulation results obtained for the different traffic compositions and sensing configurations described in Section IV. Overall, the results show that energy impacts at pedestrian crossings are primarily governed by vehicle behavior rather than propulsion technology or speed compliance. Results are reported as averages over five independent simulation runs with different random seeds. Unless stated otherwise, all relative changes in energy consumption and emissions are evaluated with respect to the baseline scenario representing 100% human-driven traffic operating under the default speed distribution (48–58 km/h). The following subsections first examine the system-level impact of autonomous vehicle penetration, followed by sensitivity analyses addressing sensing capability, speed compliance, and propulsion type.

A. EFFECT OF AV TRAFFIC PENETRATION ON ENERGY CONSUMPTION

Fig. 4 illustrates the impact of increasing AV penetration on system-level energy consumption near the unsignalized pedestrian crossing. Values represent the mean relative fuel consumption change across five stochastic simulation runs, with error bars indicating 95% confidence intervals. Results are shown for a fixed pedestrian detection range of 80 m, representing the upper bound of the considered AV sensing capabilities.

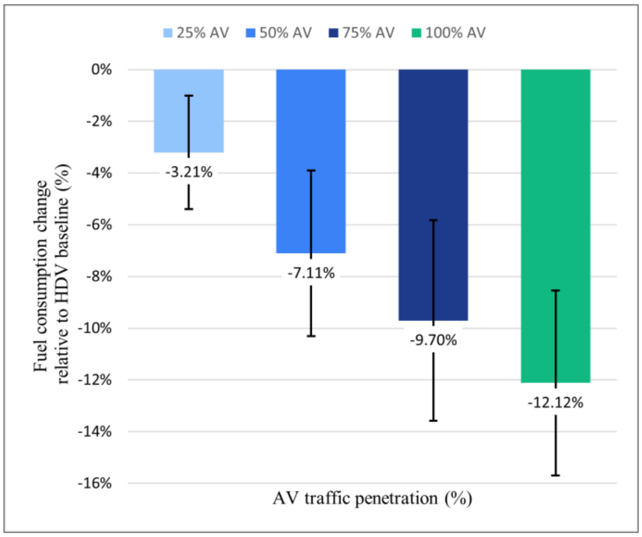

FIGURE 4. Fuel consumption change relative to HDV baseline (48-58 km/h) as a function of AV traffic penetration with 80 m detection range.

Results show a monotonic reduction in fuel consumption as AV traffic penetration increases. Even at moderate penetration levels (25–50% AVs), noticeable energy savings are observed relative to the HDV baseline. The largest reduction (12.13%) occurs under fully autonomous traffic conditions, indicating that system-level energy efficiency improves progressively during the transition from human-driven to autonomous traffic.

B. EFFECT OF PEDESTRIAN DETECTION RANGE ON ENERGY CONSUMPTION

Beyond traffic penetration, the effect of sensing capability on energy consumption was also measured. As shown in Fig. 5, longer detection ranges consistently yield lower energy use. This pattern is observed for all considered AV penetration levels.

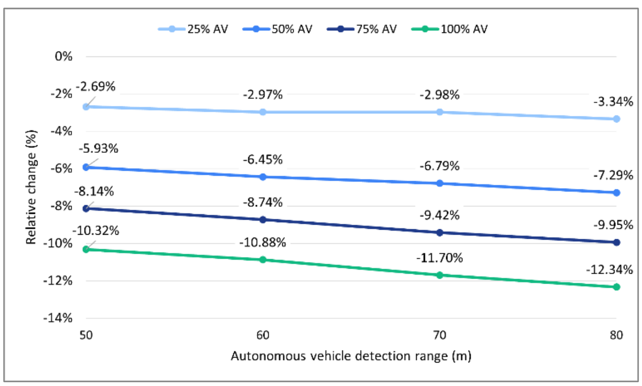

FIGURE 5. Fuel consumption change relative to the HDV baseline as a function of pedestrian detection range for different levels of AV traffic penetration.

C. INTERNAL COMBUSTION ENGINE AND ELECTRIC VEHICLE CONSUMPTION COMPARISON

To assess the robustness of the observed trends across different powertrain technologies, energy consumption changes were evaluated separately for internal combustion engine and electric vehicle models.

Fig. 6 compares the relative energy consumption changes of ICE and EV powertrains as a function of AV traffic penetration. For both propulsion types, increasing AV penetration leads to progressively larger reductions in energy consumption relative to their respective HDV baselines. The magnitude of the reduction is comparable for ICE and EV cases across all penetration levels, indicating that the energy efficiency benefits of autonomous driving are largely independent of the underlying powertrain.

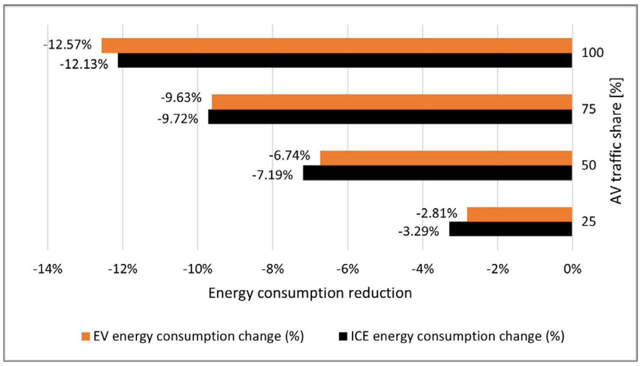

FIGURE 6. Relative energy consumption change for ICE and EV powertrains with different AV traffic penetration levels.

D. EFFECT OF SPEED COMPLIANCE ON ENERGY CONSUMPTION

To isolate the effect of speed compliance from autonomous control behavior, additional simulations were conducted in which HDVs strictly adhered to the 50 km/h speed limit.

Fig. 7 shows energy consumption changes under strict speed compliance for HDVs with those observed for autonomous driving. Enforcing a fixed speed limit for human-driven vehicles reduces energy consumption relative to the baseline case with speed variability; however, these reductions remain smaller than those achieved under autonomous control. Across all detection ranges, autonomous driving consistently yields larger energy savings, indicating that the observed benefits cannot be attributed solely to speed limit compliance.

E. TRAFFIC OPERATION AND SAFETY ANALYSIS

Beyond energy savings, the impact of the proposed speed-adaptation logic on traffic flow and safety was evaluated. The physical mechanism of the intervention is illustrated by the speed trajectories of a representative vehicle (Fig. 8). While HDVs (normal and aggressive driving style) maintain their desired speed until late in the approach, they are forced to perform abrupt deceleration as they approach the pedestrian crossing (located at the 155 m mark). In contrast, the pedestrian-aware logic enables AVs to initiate gradual speed reduction immediately upon detection. The 80 m detection range results in the smoothest transition, often allowing the vehicle to avoid a complete standstill, maintaining continuous movement at a reduced speed.

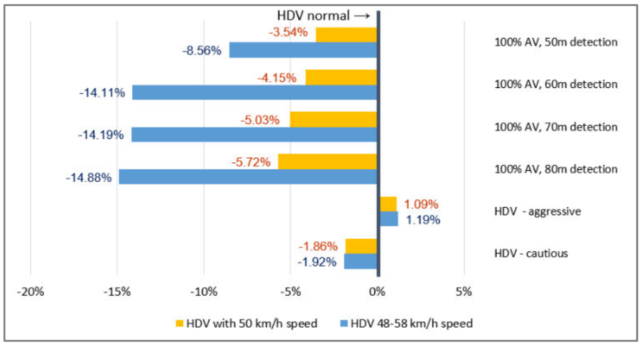

FIGURE 7. Fuel consumption change relative to the HDV baseline as a function of pedestrian detection range for different levels of AV traffic penetration.

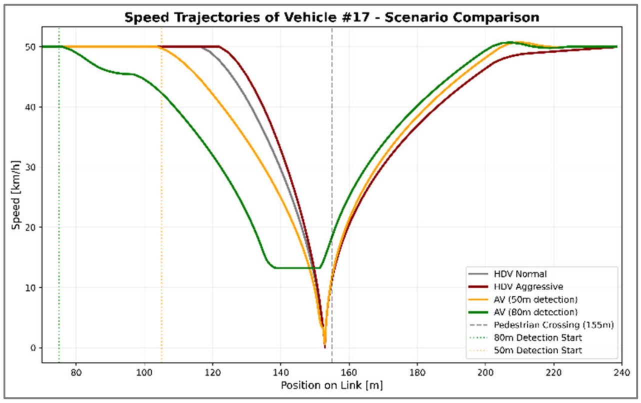

FIGURE 8. Speed trajectories of a representative vehicle across different scenarios.

This anticipatory behavior directly translates into improved road safety by smoothing the deceleration profiles. Fig. 9 presents the frequency distribution of maximum observed deceleration values across the vehicle fleet.

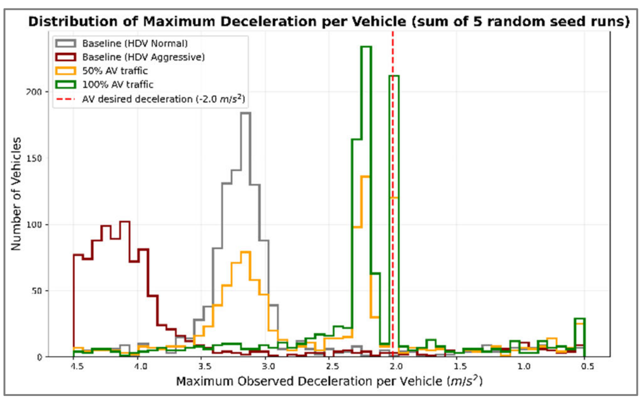

FIGURE 9. Distribution of maximum observed deceleration per vehicle (aggregated results of 5 random seed runs).

Baseline scenarios (normal and aggressive HDVs) exhibit significant peaks in the -3.0 to -4.5 m/s^2 range, representing high-risk braking maneuvers. In contrast, the 100% AV penetration scenario effectively eliminates these extreme events, with the majority of deceleration values concentrated at the -2.0 m/s^2 prescribed deceleration threshold.

The operational efficiency of the network was quantitatively confirmed by the average number of stops and network speed. The reduction in abrupt braking allowed for more fluid traffic movement; specifically, the average number of stops in the 100% AV scenario (0.598 stops/vehicle) was 13% lower than in the aggressive HDV baseline (0.687 stops/vehicle).

F. STATISTICAL SIGNIFICANCE ANALYSIS

A two-way analysis of variance (ANOVA) was performed to evaluate the effects of AV penetration rate and pedestrian detection range on energy consumption (Table 7). Normality was assessed using the Shapiro–Wilk test; minor deviations were observed in some cases but they were considered acceptable given the balanced design and the robustness of ANOVA. Effect sizes (η^2) and Tukey HSD post-hoc tests were also applied.

TABLE 7. Summary of statistical analysis results for energy consumption.

Case	Factor	F-value	η^2 (%)
1 (ICE, HDV 48-58 km/h)	AV traffic ratio	9.55^{***}	27.9
	AV detection	0.31^{ns}	0.9
2 (ICE, HDV fix 50 km/h)	AV traffic ratio	1.38^{ns}	5.3
	AV detection	0.37^{ns}	1.4
3 (EV, HDV 48-58 km/h)	AV traffic ratio	14.97^{***}	37.9
	AV detection	0.17^{ns}	0.4
4 (EV, HDV fix 50 km/h)	AV traffic ratio	$2.66^{\dagger}$	9.8
	AV detection	0.21^{ns}	0.8

*ns not significant, ***p <0.001, **p <0.01, *p <0.05, p < 0.10.*

The results indicate that AV penetration has a statistically significant effect on energy consumption in stochastic speed scenarios, namely in Case 1 (F=9.55, η^2 =27.9%) and Case 3 (F=14.97, η^2 =37.9%), with moderate to large effect sizes. In contrast, AV detection range does not show a statistically significant effect in any case, and its contribution remains negligible. Under fixed speed conditions, the effect of AV penetration is weaker and not statistically significant in Case 2 (F=1.38 η^2 =5.3%), while in Case 4 it approaches significance (F=2.66, η^2 =9.8%). These findings suggest that the observed energy savings are partly related to reduced speed variability.

Post-hoc Tukey HSD tests revealed that in stochastic HDV speed scenarios (Cases 1 and 3), significant energy savings ($p < 0.05$) are already achievable when increasing AV penetration from 25% to 75%. Notably, in these cases, the difference between 75% and 100% penetration was not statistically significant, suggesting that the majority of the flow-smoothing benefits are realized before reaching full automation. In contrast, under fixed HDV speed conditions (Case 2), no significant pairwise differences were found, while Case 4 (EV) uniquely yielded a significant reduction between 25% and 100% penetration ($p = 0.045$). This indicates that the proposed logic can exploit the high sensitivity of electric powertrains even under stable traffic conditions by mitigating minor residual speed fluctuations.

VI. DISCUSSION

This study investigated the energy consumption impacts of AVs at unsignalized pedestrian crossings under mixed traffic conditions, with particular emphasis on pedestrian-aware speed adaptation and propulsion technology. The results consistently indicate that increasing levels of AV penetration lead to reduced system-level energy consumption, primarily through smoother speed profiles and fewer abrupt deceleration and acceleration events near the crossing. Statistical analysis confirms that AV penetration is the primary factor ($p < 0.001$), with post-hoc tests showing that benefits saturate at 75% in stochastic scenarios. Notably, Case 4 (EV) uniquely yielded a significant reduction even under fixed HDV speed conditions ($p = 0.045$), while the overall effect of detection range remains statistically non-significant.

The traffic penetration-level analysis showed that energy savings emerge even at moderate AV shares (3-7%) and increase progressively toward fully autonomous traffic conditions (approximately 12%). These improvements were achieved without infrastructure support, signal coordination, or vehicle-to-infrastructure communication, indicating that behavioral adaptation alone can yield measurable system-level benefits in pedestrian-dominated urban segments.

When compared to eco-driving strategies at signalized intersections, the observed energy reductions in this study are somewhat lower but remain within a realistic range. For instance, intersection-based trajectory optimization using signal phase information has reported fuel savings of around 14% at full connected penetration [66].

Signalized intersection optimization frameworks report reductions in the range of 20–50% under idealized optimal-control assumptions [15], [26], while broader corridor-level eco-driving approaches achieved reductions of up to approximately 36%. These higher values are typically linked to coordinated speed control supported by signal information and connectivity. In contrast, the present study focused on a single unsignalized pedestrian crossing without traffic signal phase information or coordinated control, which explains the more moderate energy savings. while broader corridor-level eco-driving approaches achieved reductions of up to 36%. These higher values are typically linked to coordinated speed control supported by signal information and connectivity. In contrast, the present study focused on a single unsignalized pedestrian crossing without traffic signal phase information or coordinated control, which explains the more moderate energy savings.

Other studies investigating AV impacts in mixed traffic environments similarly emphasize the role of reduced speed variability and smoother longitudinal control in lowering fuel consumption [35]. However, most of this research concentrates on highways, platooning scenarios, or signalized intersections. Pedestrian-influenced urban segments remain less explored from an energy perspective. By explicitly modeling pedestrian-aware yielding behavior, the present study extends the discussion beyond safety considerations and quantifies its energy implications.

A previous simulation-based analysis of zebra crossings also indicated that anticipatory yielding strategies may reduce energy consumption [67], although without a structured comparison across AV penetration levels or propulsion types. The present study builds upon that work by introducing systematic scenario variation and a consistent ICE–EV comparison framework.

The sensitivity analysis shows that pedestrian detection range plays a meaningful role in enabling gradual deceleration before the crossing. Longer detection distances allow AVs to adjust speed earlier and more smoothly, thereby reducing abrupt braking events. Although the additional benefit decreases at higher detection ranges, the overall trend remains consistent across all penetration levels.

The comparison between ICE and EV propulsion indicates that the relative energy savings from autonomous control are largely independent of powertrain type. While absolute energy use differs due to drivetrain efficiency and regenerative braking characteristics, both propulsion technologies exhibit similar relative reductions as AV penetration increases. This suggests that the primary mechanism behind the observed improvements is improved speed stability rather than propulsion-specific efficiency gains consistent with observations in urban eco-driving studies [33].

From a policy perspective, the findings suggest that pedestrian-aware autonomous driving functions may contribute to incremental energy efficiency improvements in urban areas without requiring infrastructure changes. During the transitional phase of mixed traffic, measurable benefits already appear at moderate AV penetration levels, indicating that early adoption could yield environmental advantages. Furthermore, the sensitivity to detection range implies that perception performance may influence not only safety outcomes but also environmental performance, which could be relevant when defining technical requirements for urban automated driving systems.

Some limitations should be acknowledged. Pedestrian walking speeds were fixed to ensure a controlled environment; however, this excludes slower groups (e.g., elderly, children) and may underestimate AV benefits due to shorter crossing durations. The simulation framework represents a simplified unsignalized pedestrian crossing and was not calibrated to site-specific traffic conditions. HDV behavior was modeled using predefined driving profiles, which may not capture the full variability of real-world driver responses. Additionally, pedestrian detection capability was represented using fixed distance thresholds rather than detailed sensor models. While these simplifications allow controlled comparison across scenarios, they may influence the absolute magnitude of the reported energy impacts. Furthermore, unpredictable human-machine interactions, such as driver hesitation or erratic maneuvers, were not investigated in this study, which could also affect the overall energy-efficiency results.

Future research may extend this framework to network-level pedestrian interactions and cooperative AV strategies in more complex urban settings.

VII. CONCLUSION

The study demonstrated how pedestrian-aware AV control influences energy consumption at unsignalized pedestrian crossings under mixed traffic conditions. Simulation results showed that increasing AV penetration leads to measurable reductions in system-level energy use, with savings of approximately 3–7% at low to medium penetration levels and up to about 12% under fully autonomous traffic conditions.

The findings indicate that energy reductions are primarily linked to smoother and more gradual speed adjustment before the crossing, resulting in lower speed variability and fewer abrupt deceleration–acceleration events. Statistical analysis further confirmed that these effects are primarily driven by AV penetration, with no significant contribution from detection range within the examined range. The relative magnitude of these savings appears largely independent of propulsion type, as similar percentage reductions were observed for both ICE and EV. Importantly, these improvements were achieved without signal coordination or vehicle-to-infrastructure

TABLE 8. System-level fuel consumption results (L/100 km) Across AV penetration levels and detection ranges (CASE 1, ICE).

	AV detection range			
AV traffic ratio	50 m	60 m	70 m	80 m
25%	7.94	7.92	7.92	7.88
50%	7.68	7.64	7.61	7.57
75%	7.51	7.46	7.40	7.36
100%	7.33	7.28	7.22	7.16
100% HDV - cautious			8.01	
100% HDV – normal (baseline)			8.15	
100% HDV - aggressive			8.25	

TABLE 9. System-level fuel consumption results (kwh/100 km) Across AV penetration levels and detection ranges (CASE 1, EV).

AV traffic ratio	AV detection range			
	50 m	60 m	70 m	80 m
25%	19.88	19.85	19.86	19.80
50%	19.17	19.09	19.07	19.00
75%	18.66	18.57	18.48	18.41
100%	18.11	18.02	17.90	17.81
100% HDV - cautious	20.02			
100% HDV – normal (baseline)	20.37			
100% HDV - aggressive	20.87			

communication, indicating that localized behavioral control alone can contribute to urban energy efficiency.

Overall, the results suggest that pedestrian-aware AV deployment may provide incremental but consistent efficiency gains during transitional mixed-traffic phases. The proposed simulation framework offers a structured basis for evaluating additional control strategies, sensing configurations, and urban scenarios. Future research may extend the analysis toward network-level effects, cooperative driving strategies, and more detailed perception and pedestrian behavior models. In addition, incorporating stochastic sensor models could better reflect real-world variability in detection performance.

APPENDIX
DETAILED NUMERICAL RESULTS FOR CASE 1

See Tables 8 and 9.

AUTHOR STATEMENT

The authors declare no conflict of interest.

REFERENCES

[1] *Transport and Environment Report 2022-Digitalisation in the Mobility System: Challenges and Opportunities*, European Environmental Agency, Copenhagen, Denmark, 2022.

[2] Department for Transport. (2018). *Road Traffic Forecasts 2018*. Accessed: Dec. 11, 2025. [Online]. Available: https://assets.publishing.service.gov.uk/media/5e73a43d86650c2978afa311/road-traffic-forecasts-2018-document.pdf

[3] P. Capros, A. De Vita, N. Tasios, P. Siskos, M. Kannavou, A. Petropoulos, and M. Kesting, "EU reference scenario 2016-Energy, transport and GHG emissions trends to 2050," European Commission, Brussels, Belgium, Tech. Rep., 2016.

[4] S. M. Patella, F. Scrucca, F. Asdrubali, and S. Carrese, "Carbon footprint of autonomous vehicles at the urban mobility system level: A traffic simulation-based approach," *Transp. Res. D, Transp. Environ.*, vol. 74, pp. 189–200, Sep. 2019, doi: 10.1016/j.trd.2019.08.007.

[5] S. Atakishiyev, M. Salameh, H. Yao, and R. Goebel, "Explainable artificial intelligence for autonomous driving: A comprehensive overview and field guide for future research directions," *IEEE Access*, vol. 12, pp. 101603–101625, 2024, doi: 10.1109/ACCESS.2024.3431437.

[6] K. R. Reddy and A. Muralidhar, "Machine learning-based road safety prediction strategies for Internet of Vehicles (IoV) enabled vehicles: A systematic literature review," *IEEE Access*, vol. 11, pp. 112108–112122, 2023, doi: 10.1109/ACCESS.2023.3315852.

[7] H. Szűcs and J. Hézer, "Road safety analysis of autonomous vehicles: An overview," *Periodica Polytechnica Transp. Eng.*, vol. 50, no. 4, pp. 426–434, Aug. 2022, doi: 10.3311/pptr.19605.

[8] R. Hoogendoorn, B. van Arerm, and S. Hoogendoom, "Automated driving, traffic flow efficiency, and human factors: Literature review," *Transp. Res. Record, J. Transp. Res. Board*, vol. 2422, no. 1, pp. 113–120, Jan. 2014, doi: 10.3141/2422-13.

[9] J. Gonder, M. Earleywine, and W. Sparks, "Analyzing vehicle fuel saving opportunities through intelligent driver feedback," *SAE Int. J. Passenger Cars-Electron. Electr. Syst.*, vol. 5, no. 2, pp. 450–461, Apr. 2012, doi: 10.4271/2012-01-0494.

[10] D. Silva and C. Csiszár, "Locating method for pick-up and drop-off spots for shared autonomous vehicle-based mobility services," *Periodica Polytechnica Civil Eng.*, vol. 68, no. 1, pp. 197–206, 2024, doi: 10.3311/ppci.22541.

[11] S. Djavadian, R. Tu, B. Farooq, and M. Hatzopoulou, "Multi-objective eco-routing for dynamic control of connected and automated vehicles," *Transp. Res. D Transp. Environ.*, vol. 87, Oct. 2020, Art. no. 102513, doi: 10.1016/j.trd.2020.102513.

[12] Z. Yao, Y. Wang, B. Liu, B. Zhao, and Y. Jiang, "Fuel consumption and transportation emissions evaluation of mixed traffic flow with connected automated vehicles and human-driven vehicles on expressway," *Energy*, vol. 230, Sep. 2021, Art. no. 120766, doi: 10.1016/j.energy.2021.120766.

[13] F. Rossi, R. Zhang, Y. Hindy, and M. Pavone, "Routing autonomous vehicles in congested transportation networks: Structural properties and coordination algorithms," *Auton. Robots*, vol. 42, no. 7, pp. 1427–1442, 2018, doi: 10.1007/s10514-018-9750-5.

[14] S. Li, J. Li, Y. Liang, H. Zhang, S. Wu, S. Wang, and L. Cheng, "TD-SAS: A trust-aware and decentralized speed advisory system for energy-efficient autonomous vehicle platoons," *IEEE Trans. Intell. Vehicles*, vol. 9, no. 9, pp. 5554–5570, Sep. 2024, doi: 10.1109/TIV.2023.3347870.

[15] C. Sun, J. Guanetti, F. Borrelli, and S. J. Moura, "Optimal eco-driving control of connected and autonomous vehicles through signalized intersections," *IEEE Internet Things J.*, vol. 7, no. 5, pp. 3759–3773, May 2020, doi: 10.1109/JIOT.2020.2968120.

[16] M. Ghadi, "A grid-based framework for managing autonomous vehicles' movement at intersections," *Periodica Polytechnica Transp. Eng.*, vol. 52, no. 3, pp. 235–245, May 2024, doi: 10.3311/pptr.24397.

[17] L. Wang, R. Cheng, and J. Li, "Modelling of destinations for data-driven pedestrian trajectory prediction in public buildings," in *Proc. IEEE Int. Conf. Big Data (Big Data)*, Orlando, FL, USA, Dec. 2021, pp. 2450–2455, doi: 10.1109/BigData52589.2021.9671813.

[18] L. Wang, R. Cheng, and J. Li, "Modelling of pedestrian movements near an amenity in walkways of public buildings," in *Proc. 7th Int. Conf. Control Robot. (ICCAR)*, 2022, pp. 248–253, doi: 10.1109/ICCAR55106.2022.9782667.

[19] A. C. Mersky and C. Samaras, "Fuel economy testing of autonomous vehicles," *Transp. Res. C, Emerg. Technol.*, vol. 65, pp. 31–48, Apr. 2016, doi: 10.1016/j.trc.2016.01.001.

[20] M. F. Ozkan and Y. Ma, "Eco-driving of connected and automated vehicle with preceding driver behavior prediction," *J. Dyn. Syst., Meas., Control*, vol. 143, no. 1, Jan. 2021, Art. no. 011002, doi: 10.1115/1.4048108.

[21] K. Mattas, M. Makridis, P. Hallac, M. A. Raposo, C. Thiel, T. Toledo, and B. Ciuffo, "Simulating deployment of connectivity and automation on the Antwerp ring road," *IET Intell. Transp. Syst.*, vol. 12, no. 9, pp. 1036–1044, Nov. 2018, doi: 10.1049/iet-its.2018.5287.

[22] J. M. Bandeira, E. Macedo, P. Fernandes, M. Rodrigues, M. Andrade, and M. C. Coelho, "Potential pollutant emission effects of connected and automated vehicles in a mixed traffic flow context for different road types," *IEEE Open J. Intell. Transp. Syst.*, vol. 2, pp. 364–383, 2021, doi: 10.1109/OJITS.2021.3112904.

[23] C. Liu, J. Wang, W. Cai, and Y. Zhang, "An energy-efficient dynamic route optimization algorithm for connected and automated vehicles using velocity-space-time networks," *IEEE Access*, vol. 7, pp. 108866–108877, 2019, doi: 10.1109/ACCESS.2019.2933531.

[24] R. E. Stern, Y. Chen, M. Churchill, F. Wu, M. L. Delle Monache, B. Piccoli, B. Seibold, J. Sprinkle, and D. B. Work, "Quantifying air quality benefits resulting from few autonomous vehicles stabilizing traffic," *Transp. Res. D, Transp. Environ.*, vol. 67, pp. 351–365, Feb. 2019, doi: 10.1016/j.trd.2018.12.008.

[25] A. Brown, J. Gonder, and B. Repac, "An analysis of possible energy impacts of automated vehicles," in *Road Vehicle Automation*. Cham, Switzerland: Springer, 2014, ch. 2, pp. 137–153, doi: 10.1007/978-3-319-05990-7_22.

[26] X. Meng and C. G. Cassandras, "Eco-driving of autonomous vehicles for nonstop crossing of signalized intersections," *IEEE Trans. Autom. Sci. Eng.*, vol. 19, no. 1, pp. 320–331, Jan. 2022, doi: 10.1109/TASE.2020.3029452.

[27] A. Weißmann, D. Görges, and X. Lin, "Energy-optimal adaptive cruise control combining model predictive control and dynamic programming," *Control Eng. Pract.*, vol. 72, pp. 125–137, Mar. 2018, doi: 10.1016/j.conengprac.2017.12.001.

[28] T. Ercan, N. C. Onat, N. Keya, O. Tatari, N. Eluru, and M. Kucukvar, "Autonomous electric vehicles can reduce carbon emissions and air pollution in cities," *Transp. Res. D, Transp. Environ.*, vol. 112, Nov. 2022, Art. no. 103472, doi: 10.1016/j.trd.2022.103472.

[29] X. Liao, Z. Wang, X. Zhao, K. Han, P. Tiwari, M. J. Barth, and G. Wu, "Cooperative ramp merging design and field implementation: A digital twin approach based on vehicle-to-cloud communication," *IEEE Trans. Intell. Transp. Syst.*, vol. 23, no. 5, pp. 4490–4500, May 2022, doi: 10.1109/TITS.2020.3045123.

[30] Z. H. Khattak, B. L. Smith, M. D. Fontaine, J. Ma, and A. J. Khattak, "Active lane management and control using connected and automated vehicles in a mixed traffic environment," *Transp. Res. C, Emerg. Technol.*, vol. 139, Jun. 2022, Art. no. 103648, doi: 10.1016/j.trc.2022.103648.

[31] M. N. Yavuz and H. Özen, "Comprehensive evaluation of the impacts of mixed traffic conditions on urban networks," *IEEE Access*, vol. 13, pp. 73408–73429, 2025, doi: 10.1109/ACCESS.2025.3563785.

[32] E. Jungblut, T. Grube, J. Linssen, and D. Stolten, "Fuel-saving opportunities for automated vehicles: A driving cycle analysis," *Transp. Res. Interdiscipl. Perspect.*, vol. 22, Nov. 2023, Art. no. 100964, doi: 10.1016/j.trip.2023.100964.

[33] R. Lot, J. Fleming, B. Chen, and S. Evangelou, "Eco-driving optimal control for electric vehicles with driver preferences," *Transp. Eng.*, vol. 19, Mar. 2025, Art. no. 100302, doi: 10.1016/j.treng.2025.100302.

[34] X. T. Yang, K. Huang, Z. Zhang, Z. A. Zhang, and F. Lin, "Eco-driving system for connected automated vehicles: Multi-objective trajectory optimization," *IEEE Trans. Intell. Transp. Syst.*, vol. 22, no. 12, pp. 7837–7849, Dec. 2021, doi: 10.1109/TITS.2020.3010726.

[35] I. Mahdinia, R. Arvin, A. J. Khattak, and A. Ghiasi, "Safety, energy, and emissions impacts of adaptive cruise control and cooperative adaptive cruise control," *Transp. Res. Record: J. Transp. Res. Board*, vol. 2674, no. 6, pp. 253–267, Jun. 2020, doi: 10.1177/0361198120918572.

[36] J. V. S. Busch, V. Latzko, M. Reisslein, and F. H. P. Fitzek, "Optimised traffic light management through reinforcement learning: Traffic state agnostic agent vs. holistic agent with current V2I traffic state knowledge," *IEEE Open J. Intell. Transp. Syst.*, vol. 1, pp. 201–216, 2020, doi: 10.1109/OJITS.2020.3027518.

[37] M. Wegener, L. Koch, M. Eisenbarth, and J. Andert, "Automated eco-driving in urban scenarios using deep reinforcement learning," *Transp. Res. Part C: Emerg. Technol.*, vol. 126, May 2021, Art. no. 102967, doi: 10.1016/j.trc.2021.102967.

[38] J. Liu, W. Zhao, and C. Xu, "An efficient on-ramp merging strategy for connected and automated vehicles in multi-lane traffic," *IEEE Trans. Intell. Transp. Syst.*, vol. 23, no. 6, pp. 5056–5067, Jun. 2022, doi: 10.1109/TITS.2020.3046643.

[39] Z. Chen and X. Huang, "Pedestrian detection for autonomous vehicle using multi-spectral cameras," *IEEE Trans. Intell. Vehicles*, vol. 4, no. 2, pp. 211–219, Jun. 2019, doi: 10.1109/TIV.2019.2904389.

[40] M. Dimitrievski, P. Veelaert, and W. Philips, "Behavioral pedestrian tracking using a camera and LiDAR sensors on a moving vehicle," *Sensors*, vol. 19, no. 2, p. 391, 2019, doi: 10.3390/s19020391.

[41] M. Schratter, M. Hartmann, and D. Watzenig, "Pedestrian collision avoidance system for autonomous vehicles," *SAE Int. J. Connected Automated Vehicles*, vol. 2, no. 4, pp. 279–293, Dec. 2019, doi: 10.4271/12-02-04-0021.

[42] A. Brunoud, A. Lombard, M. Zhang, A. Abbas-Turki, N. Gaud, and A. Koukam, "Comparison of deep reinforcement learning methods for safe and efficient autonomous vehicles at pedestrian crossings," in *Proc. IEEE 25th Int. Conf. Intell. Transp. Syst. (ITSC)*, Macau, Oct. 2022, pp. 2556–2562, doi: 10.1109/ITSC55140.2022.9921781.

[43] S. Zamboni, Z. T. Kefato, S. Girdzijauskas, C. Norén, and L. Dal Col, "Pedestrian trajectory prediction with convolutional neural networks," *Pattern Recognit.*, vol. 121, Jan. 2022, Art. no. 108252, doi: 10.1016/j.patcog.2021.108252.

[44] M. Prédhumeau, L. Mancheva, J. Dugdale, and A. Spalanzani, "Agent-based modeling for predicting pedestrian trajectories around an autonomous vehicle," *J. Artif. Intell. Res.*, vol. 73, pp. 1385–1433, Apr. 2022, doi: 10.1613/jair.1.13425.

[45] N. Ling, Q. Wang, B. Chen, Y. B. Zhao, and Y. Zhang, "Eco-driving decision making based on V2X communication and spatio-temporal prediction of pedestrians," *IEEE Trans. Intell. Transp. Syst.*, vol. 26, no. 8, pp. 11905–11915, Aug. 2025, doi: 10.1109/TITS.2025.3568195.

[46] H. Tu, L. Zhao, R. Tu, and H. Li, "The energy-saving effect of early-stage autonomous vehicles: A case study and recommendations in a metropolitan area," *Energy*, vol. 297, Jun. 2024, Art. no. 131274, doi: 10.1016/j.energy.2024.131274.

[47] B. Yang, S. Yan, Z. Wang, and K. Nakano, "Prediction based trajectory planning for safe interactions between autonomous vehicles and moving pedestrians in shared spaces," *IEEE Trans. Intell. Transp. Syst.*, vol. 24, no. 10, pp. 10513–10524, Oct. 2023, doi: 10.1109/TITS.2023.3281157.

[48] J. Wang, H. Zhang, B. Wu, and W. Liu, "Symmetry-guided electric vehicles energy consumption optimization based on driver behavior and environmental factors: A reinforcement learning approach," *Symmetry*, vol. 17, no. 6, p. 930, Jun. 2025, doi: 10.3390/sym17060930.

[49] S. Szigeti, "Dataset and control algorithm for pedestrian-aware speed adaptation of autonomous vehicles at unsignalized crossings," *IEEE Dataport*, Feb. 17, 2026, doi: 10.21227/zc59-ar79.

[50] R. Zhang and S. Cao, "Extending reliability of mmWave radar tracking and detection via fusion with camera," *IEEE Access*, vol. 7, pp. 137065–137079, 2019, doi: 10.1109/ACCESS.2019.2942382.

[51] S. Li, K. Geng, G. Yin, Z. Wang, and M. Qian, "MVMM: Multi-view multimodal 3-D object detection for autonomous driving," *IEEE Trans. Ind. Informat.*, vol. 20, no. 1, pp. 845–853, Jan. 2024, doi: 10.1109/TII.2023.3263274.

[52] S. Adnan Yusuf, A. Khan, and R. Souissi, "Vehicle-to-everything (V2X) in the autonomous vehicles domain—A technical review of communication, sensor, and AI technologies for road user safety," *Transp. Res. Interdiscipl. Perspect.*, vol. 23, Jan. 2024, Art. no. 100980, doi: 10.1016/j.trip.2023.100980.

[53] European Automobile Manufacturers Association. (2024). *Differences Between Diesel and Petrol*. Accessed: Dec. 6, 2025. [Online]. Available: https://www.acea.auto/fact/differences-between-diesel-and-petrol/

[54] A. Albatayneh, M. N. Assaf, D. Alterman, and M. Jaradat, "Comparison of the overall energy efficiency for internal combustion engine vehicles and electric vehicles," *Environ. Climate Technol.*, vol. 24, no. 1, pp. 669–680, Jan. 2020, doi: 10.2478/rtuect-2020-0041.

[55] H. Togun, A. Basem, T. Abdulrazzaq, N. Biswas, A. M. Abed, J. M. Dhabab, A. Chattopadhyay, K. Slimi, D. Paul, P. Barmavatu, and A. Chrouda, "Development and comparative analysis between battery electric vehicles (BEV) and fuel cell electric vehicles (FCEV)," *Appl. Energy*, vol. 388, Jun. 2025, Art. no. 125726, doi: 10.1016/j.apenergy.2025.125726.

[56] C. Yang, T. Sun, W. Wang, Y. Li, Y. Zhang, and M. Zha, ‘‘Regenerative braking system development and perspectives for electric vehicles: An overview,’’ *Renew. Sustain. Energy Rev.*, vol. 198, Jul. 2024, Art. no. 114389, doi: 10.1016/j.rser.2024.114389.

[57] N. M. Jamadar and H. T. Jadhav, ‘‘A review on braking control and optimization techniques for electric vehicle,’’ *Proc. Inst. Mech. Eng., D, J. Automobile Eng.*, vol. 235, no. 9, pp. 2371–2382, Aug. 2021, doi: 10.1177/0954407021996906.

[58] X. Zhang, D. Gohlich, and J. Li, ‘‘Energy-efficient toque allocation design of traction and regenerative braking for distributed drive electric vehicles,’’ *IEEE Trans. Veh. Technol.*, vol. 67, no. 1, pp. 285–295, Jan. 2018, doi: 10.1109/TVT.2017.2731525.

[59] S. Heydari, P. Fajri, M. Rasheduzzaman, and R. Sabzehgar, ‘‘Maximizing regenerative braking energy recovery of electric vehicles through dynamic low-speed cutoff point detection,’’ *IEEE Trans. Transport. Electrific.*, vol. 5, no. 1, pp. 262–270, Mar. 2019, doi: 10.1109/TTE.2019.2894942.

[60] H. I. Ashqar, M. Obaid, A. Jaber, R. Ashqar, N. O. Khanfar, and M. Elhenawy, ‘‘Incorporating driving behavior into vehicle fuel consumption prediction: Methodology development and testing,’’ *Discover Sustainability*, vol. 5, no. 1, p. 344, Oct. 2024, doi: 10.1007/s43621-024-00511-z.

[61] E. Fiani, U. Karl, G. Umlauf, J. De Assunçao, S. Kakareka, and H. Fiedler. (2013). *Toolkit for Identification and Quantification of Releases of Dioxins, Furans and Other Unintentional POPs*. United Nations Environment Programme, Geneva, Switzerland. Accessed: Dec. 7, 2025. [Online]. Available: https://toolkit.pops.int/Publish/Downloads/UNEP-POPS-TOOLKIT-2012-En.pdf

[62] *MEP/EEA Air Pollutant Emission Inventory Guidebook 2023: Technical Guidance To Prepare National Emission Inventories*, European Environment Agency, Copenhagen, Denmark, 2023.

[63] J. Buberger, A. Kersten, M. Kuder, R. Eckerle, T. Weyh, and T. Thiringer, ‘‘Total CO_2-equivalent life-cycle emissions from commercially available passenger cars,’’ *Renew. Sustain. Energy Rev.*, vol. 159, May 2022, Art. no. 112158, doi: 10.1016/j.rser.2022.112158.

[64] J. Ejsmont, G. Ronowski, L. Ydrefors, W. Owczarzak, S. Sommer, and B. Świeczko-Żurek, ‘‘Comparison of tire rolling resistance measuring methods for different surfaces,’’ *Int. J. Automot. Technol.*, vol. 25, no. 4, pp. 965–976, Aug. 2024, doi: 10.1007/s12239-024-00092-w.

[65] M. G. Connolly, A. Ivankovic, and M. J. O’Rourke, ‘‘Drag reduction technology and devices for road vehicles—A comprehensive review,’’ *Heliyon*, vol. 10, no. 13, Jul. 2024, Art. no. e33757, doi: 10.1016/j.heliyon.2024.e33757.

[66] H. Yang, F. Almutairi, and H. Rakha, ‘‘Eco-driving at signalized intersections: A multiple signal optimization approach,’’ *IEEE Trans. Intell. Transp. Syst.*, vol. 22, no. 5, pp. 2943–2955, May 2021, doi: 10.1109/TITS.2020.2978184.

[67] S. Szigeti, D. Földes, and X. Ye, ‘‘Simulating the alteration in energy consumption at a zebra crossing considering different traffic rates of electric and rule-following autonomous vehicles,’’ *Acta Technica Jaurinensis*, vol. 16, no. 4, pp. 174–182, Nov. 2023, doi: 10.14513/actatechjaur.00722.

SZILÁRD SZIGETI received the M.Sc. degree in transportation engineering, in 2017. He is currently pursuing the Ph.D. degree with the Department of Transport Technology and Economics, Budapest University of Technology and Economics. His master’s thesis focused on the operational model of an autonomous flexible public transport systems. He is a Researcher with the Institute for Transport Sciences, where he represents the institute in international professional organizations related to road traffic safety. He has authored 25 scientific publications, including six papers indexed in the Web of Science Core Collection, with 23 Web of Science citations. His main research interests include road traffic safety, autonomous vehicle-based mobility systems, traffic simulation, and transport system optimization.

GÁBOR PAUER received the Ph.D. degree in transportation engineering from Budapest University of Technology and Economics. He is the Head of the Traffic Safety and Traffic Engineering Research Centre, Institute for Transport Sciences (KTI), Hungary. He has extensive experience in leading and implementing national and international research projects, preparing safety analyses and international benchmarks, and supporting strategic decision-making and action plan development. He represents Hungary in several international road safety organizations and working groups. His work integrates data-driven analysis, behavioral research, and infrastructure safety assessment to support evidence-based transport policy and innovation. His research interests include traffic safety, human behavior in transport systems, infrastructure safety, and autonomous vehicles.

DÁVID FÖLDES received the Ph.D. degree (summa cum laude) in transportation science, in 2019. His Ph.D. dissertation titled ‘‘Development of Innovative Transport Systems and Mobility Services’’. He is a Research Associate with the Department of Transport Technology and Economics, Budapest University of Technology and Economics. Since 2021, he has been a Ph.D. Supervisor for students in transportation science. He has been involved in several national and international research projects. He has more than 100 scientific publications, with over 450 independent Web of Science citations. His research interests include micromobility, shared mobility, electromobility, and mobility services based on autonomous vehicles, with particular emphasis on travelers’ habits and expectations. He won the European Friedrich-List Award 2020 in the category Ph.D. dissertation.